Supporting Information

Systematic Investigation of Urea Containing Sidechains in Electrochromic ProDOT and EDOT Copolymers

Md Mahmudul Hasan,[a] Raul S. Ramos,[a] Kavish Saini,[a] Md Shahjahan Mahmud,[b] Ashley Morales[a], Adrian Bocanegra Richarte,[a] Michael Lyubchenko,[c] Sreeprasad T. Sreenivasan,[a] Yirong Lin[b] and Robert M. Pankow[a]*

[a]Department of Chemistry and Biochemistry, University of Texas at El Paso, El Paso, Texas 79968, USA.

[b]Department of Aerospace and Mechanical Engineering, University of Texas at El Paso, El Paso, Texas 79968, USA.

[c]Department of Metallurgical, Materials and Biomedical Engineering, University of Texas at El Paso, El Paso, Texas 79968, USA.

*To whom correspondence may be addressed:

R. M. P. (rmpankow@utep.edu)

Table of Contents

1. General.

All reactions were performed under dry N_2 in oven dried glassware, unless otherwise noted. All reagents and solvents were purchased and used as received from commercial sources: Fisher Scientific, VWR, Ambeed, and Sigma Aldrich. Monomers **S7** and **S8** were synthesized following literature procedure.[1]

NMR were recorded at 25 °C using $CDCl_3$ or at 80 °C using $C_2D_2Cl_4$ on a 400 MHz Bruker Avance III. All spectra were referenced to $CHCl_3$ (7.26 ppm) or C_2DHCl_4 (6.00 ppm). ESI-HRMS was performed on a JEOL AccuTOF TC-100 using HPLC grade MeOH or THF for monomers and calibrated to PEG 600. A Thermo Nicolet iS5 FTIR spectrometer (Thermo Fisher Scientific, MA, USA) was operated for the monomers and polymers. Samples were measured directly in solid state using an attenuated total reflectance (ATR) accessory. Prior to data acquisition, a background spectrum was recorded under identical conditions and subtracted automatically from the sample spectra. Spectra were recorded with parameters including a wavenumber range from 4000 to 400 $cm^{-1,}$ a resolution of 4 cm^{-1} , and an average of 16 scans at room temperature.[2]

Thermogravimetric analysis (TGA) measurements were performed using a Mettler Toledo TGA/DSC 1 (temperature range of 40-750 °C at 10 dpm) in alumina crucibles charged with 2-3 mg of polymer sample under a flow of N_2 protective gas (20 mL/min) and dry compressed air reactive gas (10 mL/min) to facilitate combustion. Differential scanning calorimetry (DSC) measurements were performed using a TA Instruments DSC 25 equipped with a RCS 90 chiller under UHP-N_2. Samples were prepared by sealing ~7 mg of polymer in Al-pans with the recorded traces provided from the second heating cycle.

Electrochemical measurements (CV and scan rate dependency) were performed using the polymer coated glass-ITO substrate as the working electrode, Ag-wire as the counter electrode, and Ag-wire as the reference electrode with 0.1 M $LiPF_6$/PC as the supporting electrolyte. All measurements were referenced to Fc/Fc^+, and the polymer films were subjected to electrochemical conditioning (cycling -1.0 to +1.0 V 10x) prior to measurement. Spectroelectrochemistry and electrochromic switching measurements were performed using polymer coated glass-ITO substrates submerged in 0.5 M $LiPF_6$/PC electrolyte using a Ag-wire psuedoreference and counter electrode.

2. Monomer Synthesis.

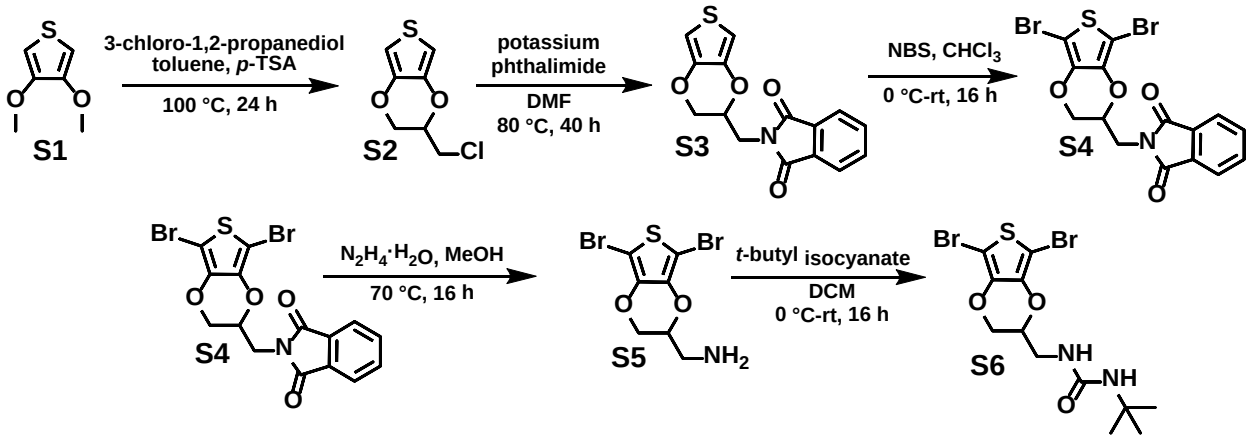

Scheme S1. Monomer synthesis.

2-chloromethyl-3,4-ethylenedioxythiophene (S2). A 500 mL round-bottom flask equipped with a stir bar and condenser was cooled under nitrogen and vacuum-backfilled with nitrogen 3x. **S1** (2.0 g, 13.9 mmol, 1 equiv.), 3-chloro-1,2-propanediol (6.13 g, 55.5 mmol, 4 equiv.), and p-tolyl sulfonic acid (234 mg, 1.39 mmol, 0.1 equiv.) were dissolved in toluene (140 mL) and degassed with nitrogen for 20 minutes. Then, the reaction mixture was heated for 24 h at 100 °C under a nitrogen atmosphere. A solvent bulb filled with 4 Å molecular sieves was placed on top of the condenser during the assembly of the reaction apparatus. The reaction mixture was then cooled to room temperature, and the toluene was removed *en vacuo*. DI-H_2O (50 mL) was then added and the mixture was extracted with diethyl ether (3x50 mL). The organic portion was washed with brine three times. Then, it was dried over $MgSO_4$ with activated charcoal. After concentrating the residue under vacuum, the crude product was purified by column chromatography on silica gel using 40% DCM/hexanes (*v:v*) to obtain the product as a white solid in 40% yield. ^{1}H-NMR ($CDCl_3$, 25 °C, 400 MHz): δ (ppm) 6.37(s, 2H), 4.40 – 4.35 (m, 1H), 4.30 – 4.26 (dd, J = 2.3, 11.7 Hz, 1H), 4.18 – 4.13 (q, J = 6.28 Hz,1H), 3.75–3.64 (m, 2H). ^{13}C-NMR (100 MHz, $CDCl_3$): δ (ppm) 141.11, 140.66, 100.13, 100.12, 72.83, 65.55, 41.30. Consistent with literature reports.[3]

2-[2,3-Dihydrothieno[3,4-b]-1,4-dioxin-2-yl) methyl]-1H-isoindole-1,3(2H)-dione (S3). A 100 mL round-bottom flask equipped with a stirbar was charged with **S2** (1.0 g, 5.24 mmol, 1 equiv.) and potassium phthalimide (1.94g, 10.5 mmol, 2 equiv.). Anhydrous DMF (48 ml) was then added and the reaction mixture was heated for 40 h at 80 °C under nitrogen atmosphere. The reaction

mixture was then cooled to room temperature and DI-H_2O (~25 mL) was added. The precipitate was collected via vacuum filtration and washed with a copious amount of DI-H_2O. The product is then dried under vacuum 24 hours and used without further purification. 72% yield. ^{1}H-NMR ($CDCl_3$, 25 °C, 400 MHz): δ (ppm) 7.89 – 7.87 (dd, *J* = 2.8, 5.6 Hz, 2H), 7.76 – 7.73 (dd, *J* = 2.8, 5.6 Hz, 2H), 6.33 – 6.31 (m, 2H), 4.52 – 4.46 (m, 1H), 4.27 – 4.23 (dd, *J* = 4.0, 12.0 Hz, 1H), 4.10 – 4.00 (m, 2H), 3.90 – 3.86 (dd, *J* = 4.0, 12.0 Hz, 1H) . ^{13}C-NMR (100 MHz, $CDCl_3$): δ (ppm) 167.93, 141.10, 140.79, 134.21, 131.86, 123.52, 100.25, 99.86, 71.13, 66.31, 37.89. Consistent with literature reports.[3]

2-[2,3-Dibromothieno[3,4-b]-1,4-dioxin-2-yl) methyl]-1H-isoindole-1,3(2H)-dione (S4). A 250 mL round-bottom flask shield with Al-foil was charged with **S4** (1.00 g, 3.32 mmol, 1 equiv.) and anhydrous $CHCl_3$ (166 mL) under a nitrogen atmosphere. Then, the mixture was degassed with nitrogen for 15 minutes and cooled to 0 °C. NBS (1.47g, 8.3 mmol, 2.5 equiv.) was then added portion-wise over 1 h. The reaction mixture was then brought to room temperature and stirred overnight by covering. Excess NBS was quenched via the slow addition of saturated aqueous sodium bisulfate. The crude mixture was then extracted with $CHCl_3$, washed with brine 2 times and dried with Na_2SO_4. The solvent was removed under reduced pressure, and the crude product was purified by recrystallization with MeOH. 60% yield. ^{1}H-NMR ($CDCl_3$, 25 °C, 400 MHz) δ (ppm): 7.90 – 7.87 (dd, *J* = 2.8, 5.6 Hz, 2H), 7.76 – 7.74 (dd, *J* = 2.8, 5.6 Hz, 2H), 4.58 – 4.52 (m, 1H), 4.34 – 4.30 (dd, *J* = 2.4, 12.0 Hz 1H), 4.15 – 4.09 (m, 2H), 3.92 – 3.87 (dd, *J* = 5.6, 16.0 Hz 1H) . ^{13}C-NMR (100 MHz, $CDCl_3$): δ (ppm) 167.76, 139.05, 138.61, 134.29, 131.81, 123.57, 86.31, 85.77, 71.44, 66.44, 37.56. ATR-FTIR (neat) cm^{-1}: 2922 (w) , 1700 (s), 1503 (m), 1394 (m), 1368 (m), 1027 (s).

5,7-dibromo-2,3-dihydro-Thieno[3,4-b]-1,4-dioxin-2-methanamine (S5). **S4** (1.00 g, 2.28 mmol, 1 equiv.) was added to a 2-neck 50 mL round-bottom flask equipped with a stir-bar and condenser and dissolved in MeOH (15 mL). Hydrazine monohydrate (330 mg, 6.53 mmol, 3 equiv.) was then added dropwise at room temperature. The reaction mixture was then stirred at 70 °C for 24 h. The reaction was then cooled to room temperature and the MeOH was removed via distillation. Aqueous 10% KOH (10 mL) and 10 ml of DCM was added to the reaction mixture and stirred for 20 min at room temperature. The mixture was extracted with DCM, washed with brine, and dried with Na_2SO_4. The crude product was then purified using column chromatography on Si-gel with

12.5% MeOH/ DCM (*v:v*). 62% yield. ^{1}H-NMR ($CDCl_3$, 25 °C, 400 MHz): δ (ppm) 4.29 – 4.25 (dd, *J* = 2.0, 12.0 Hz 1H), 4.16 – 4.11 (m, 1H), 4.07 – 4.02 (dd, *J* = 7.8, 11.6 Hz 1H), 3.00 – 2.97 (m, 2H), 1.40 (s, 2H). ^{13}C-NMR (100 MHz, $CDCl_3$): δ (ppm) 139.54, 139.48, 85.29, 85.25, 75.68, 66.77, 41.86.

1,1-Dimethylethyl N-[(5,7-dibromo-2,3-dihydrothieno[3,4-b]-1,4-dioxin-2-yl)methyl]urea (S6). A 50 ml oven-dried two-neck round-bottom flask equipped with a stir-bar was charged with **S5** (0.66 g, 2 mmol, 1 equiv.) and anhydrous DCM (5 mL). Then, the mixture was degassed with nitrogen for 15 min and cooled to 0 °C. Tert-butyl isocyanate (200 mg, 2 mmol, 1 equiv.) was then added dropwise, and the reaction mixture was stirred for 30 minutes at 0 °C before removing the ice-bath followed by stirring at room-temperature for 16 h. The DCM was then removed *en vacuo*, and the residue was purified using column chromatography on Si-gel with 5% MeOH/DCM (*v:v*). 65% yield. ^{1}H-NMR ($CDCl_3$, 25 °C, 400 MHz): δ (ppm) 4.51 – 4.48 (t, *J* = 8.0 Hz, 1H), 4.35 – 4.31 (dd, *J* = 4.0 Hz, 12.0 Hz, 1H), 4.28 - 4.24 (m, 2H) , 4.01-3.96 (dd, *J* = 8.0 Hz, 10.0 Hz, 1H), 3.60 – 3.54 (m, 1H), 3.52 – 3.45 (m,1H), 1.34 (s, 9H) . ^{13}C-NMR (100 MHz, $CDCl_3$): δ (ppm) 156.88, 139.53, 139.44, 85.56, 85.34, 74.27, 66.72, 50.65, 39.87, 29.44. ATR-FTIR (neat) cm^{-1}: 3319 (br, w), 2964 (w), 1632 (m), 1502 (m), 1360 (m), 1056 (m). ESI-HRMS (*m/z*) calculated: 428.14; found [M^+]: 428.29.

3. Monomer NMR.

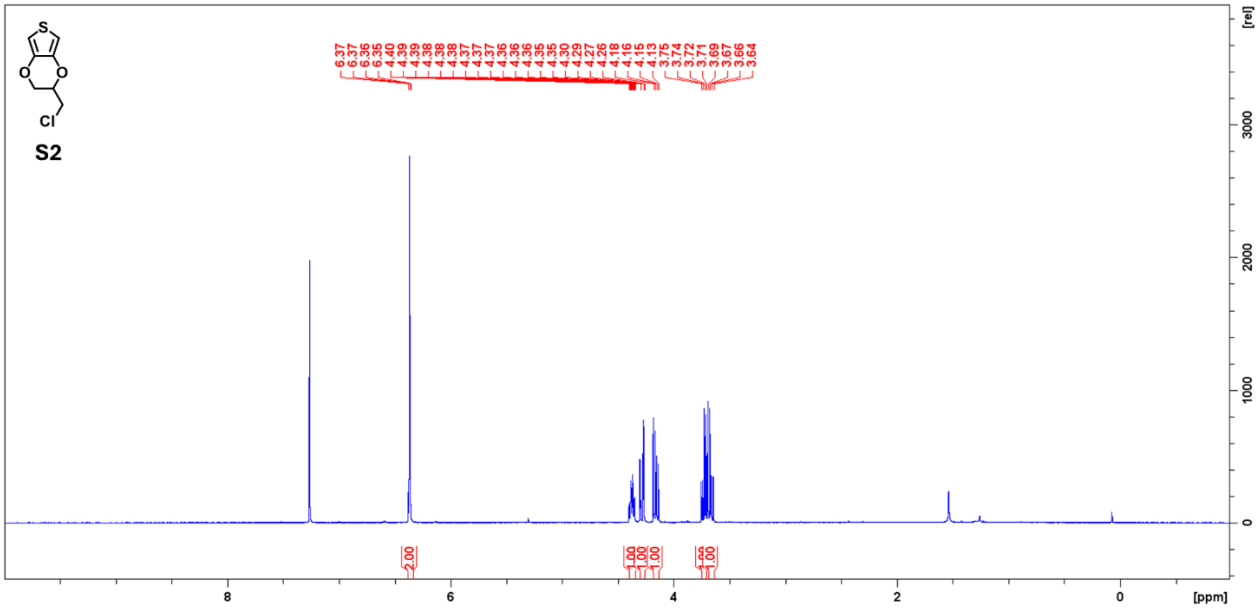

Figure S1. ^{1}H-NMR of S2 collected in $CDCl_3$ at 25 °C and 400 MHz.

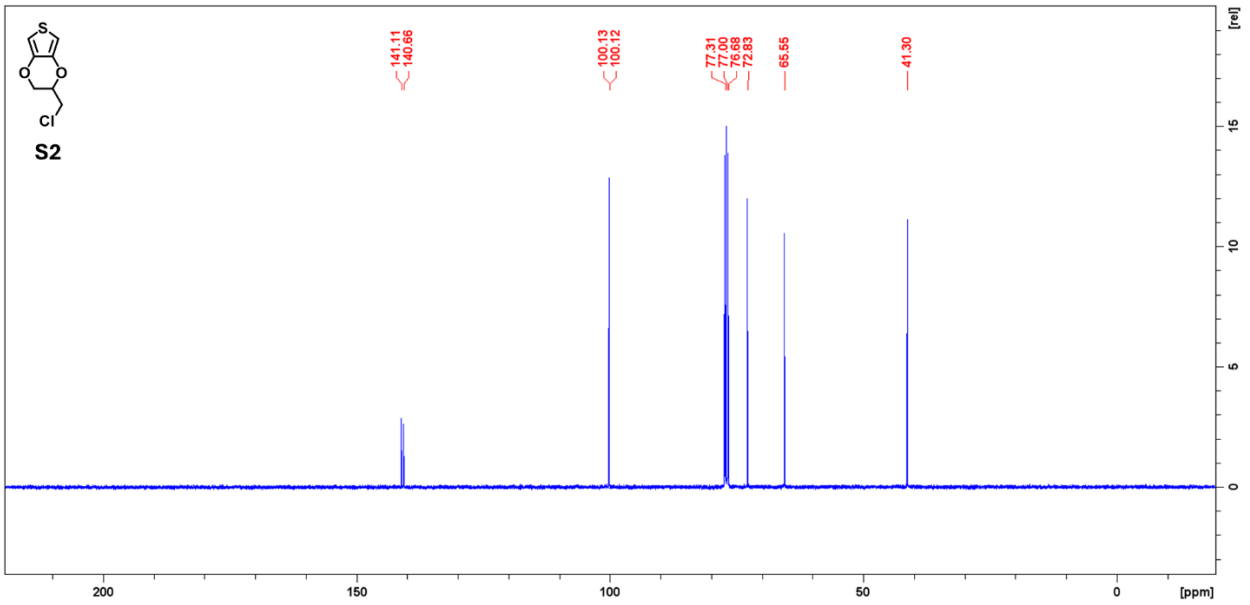

Figure S2. ^{13}C-NMR of S2 collected in $CDCl_3$ at 25 °C and 100 MHz.

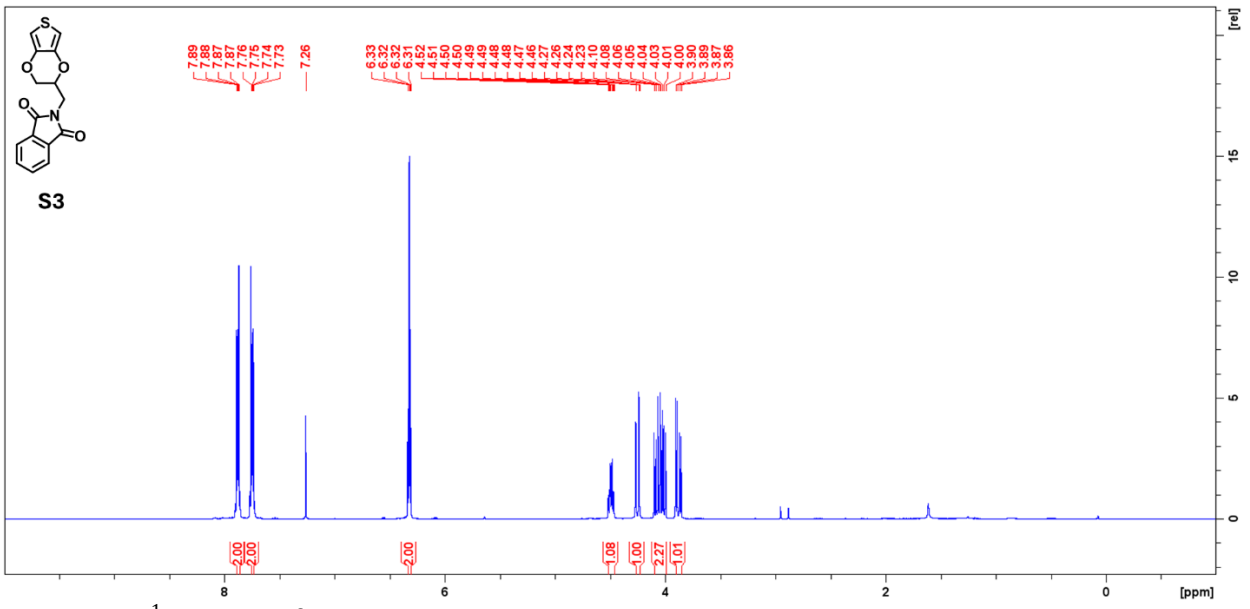

Figure S3. ^{1}H-NMR of S3 collected in $CDCl_3$ at 25 °C and 400 MHz.

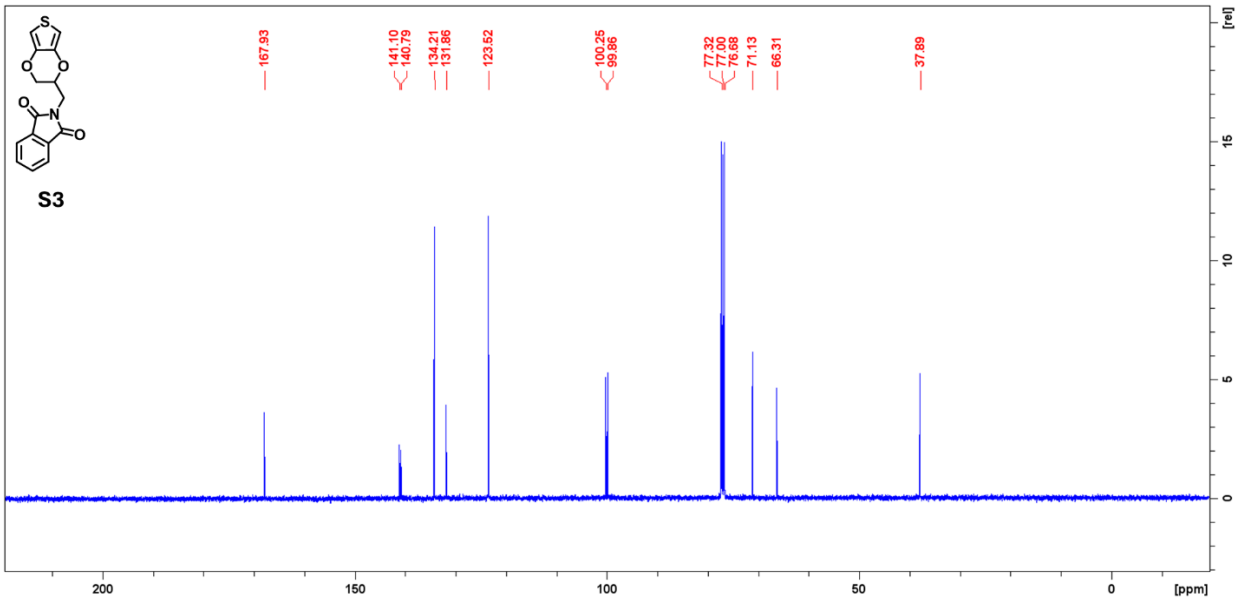

Figure S4. ^{13}C-NMR of S3 collected in $CDCl_3$ at 25 °C and 100 MHz.

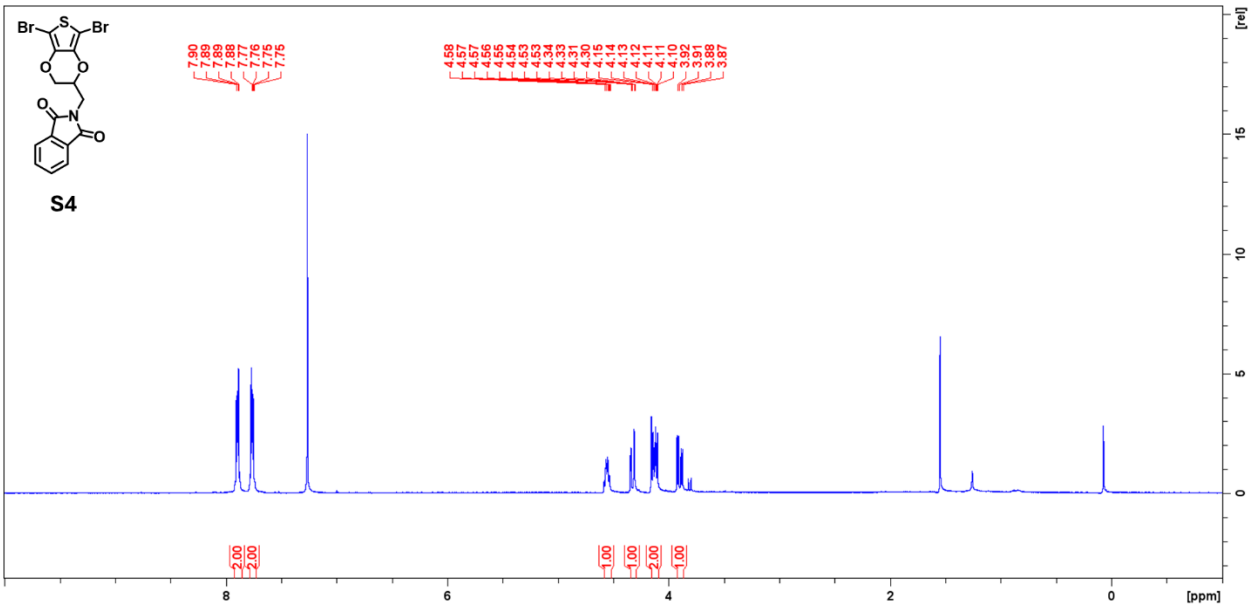

Figure S5. ^{1}H-NMR of S4 collected in $CDCl_3$ at 25 °C and 400 MHz.

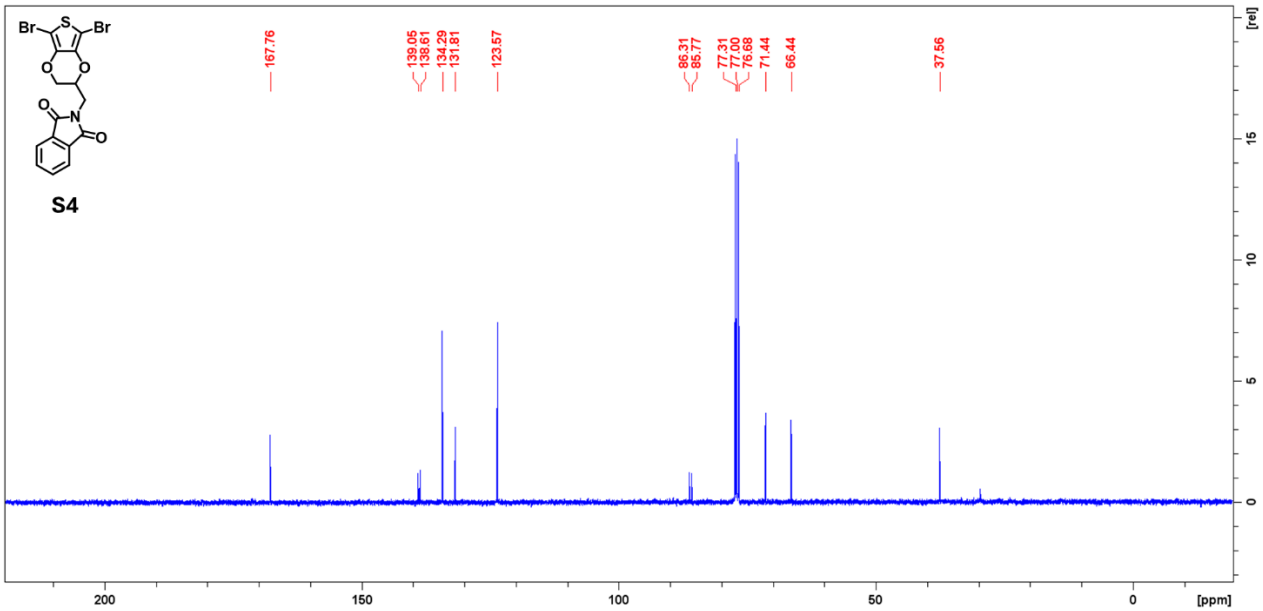

Figure S6. ^{13}C-NMR of S4 collected in $CDCl_3$ at 25 °C and 100 MHz.

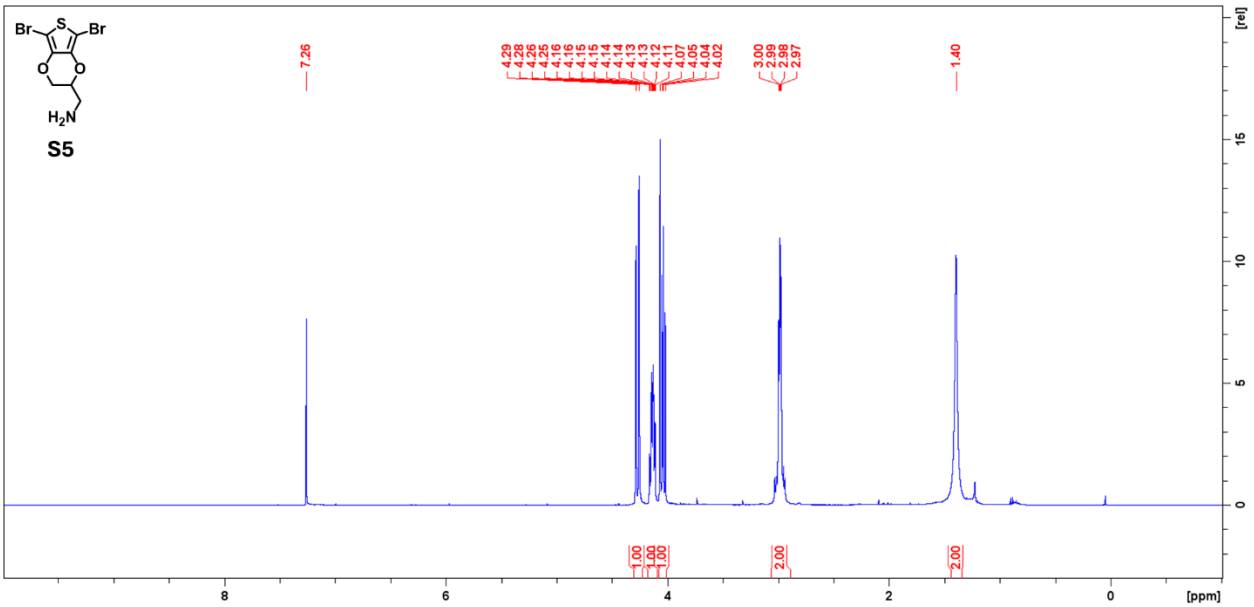

Figure S7. ^{1}H-NMR of S5 collected in $CDCl_3$ at 25 °C and 400 MHz.

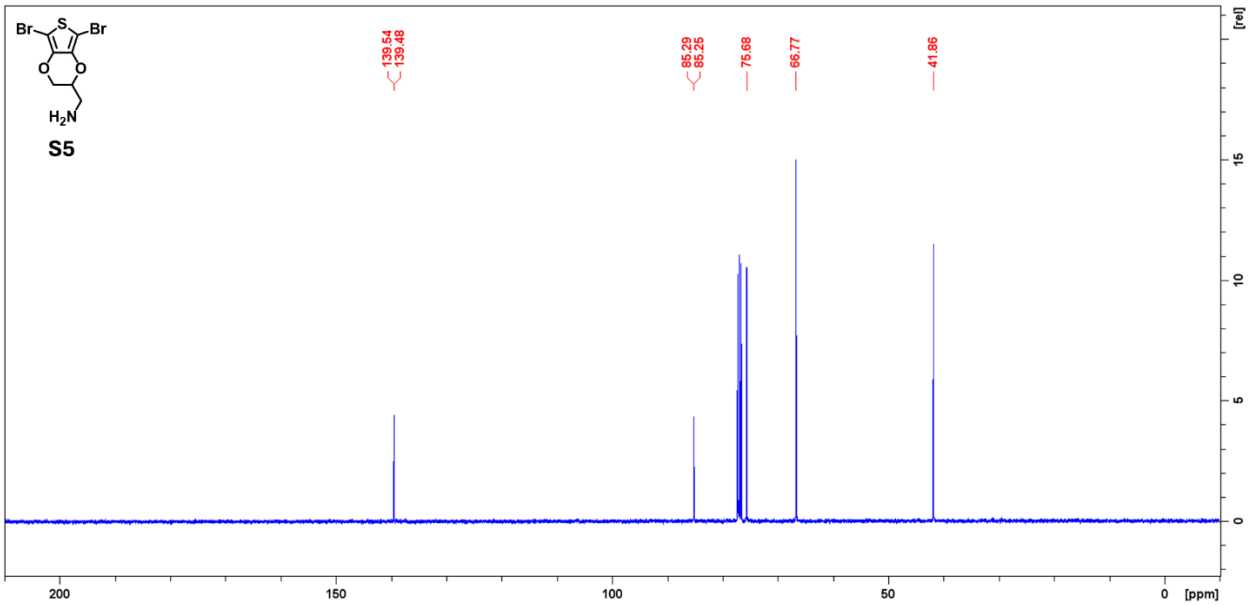

Figure S8. ^{13}C-NMR of S5 collected in $CDCl_3$ at 25 °C and 100 MHz.

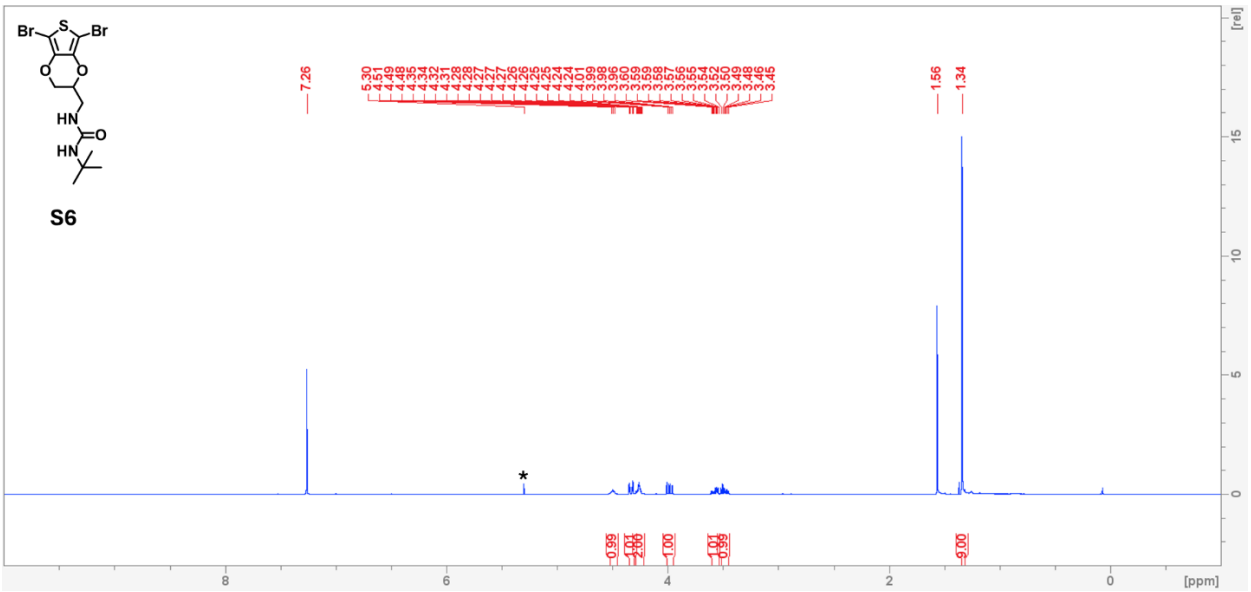

Figure S9. ^{1}H-NMR of S6 collected in $CDCl_3$ at 25 °C and 400 MHz. *Indicates residual solvent (DCM).

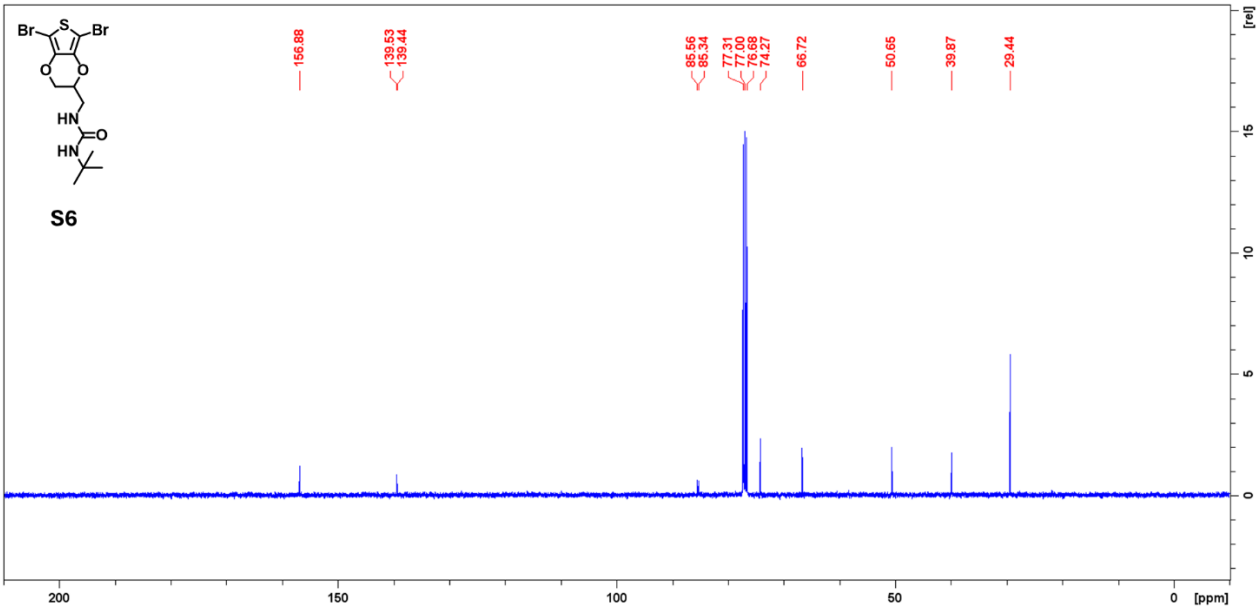

Figure S10. ^{13}C-NMR of S6 collected in $CDCl_3$ at 25 °C and 100 MHz.

4. Monomer ATR-FTIR.

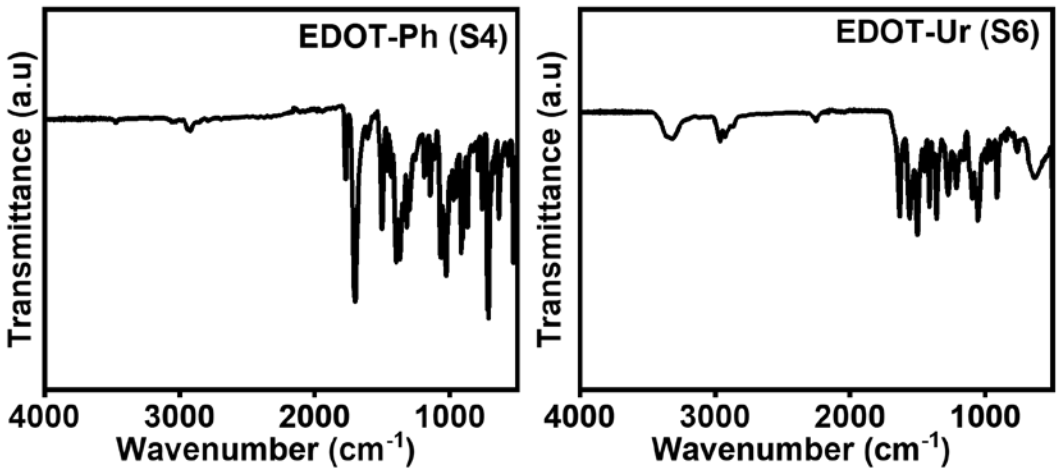

Figure S11. ATR-FTIR spectra of S4 (left) and S6 (right).

Table S1.

Entry	N-H (cm^{-1})	C-H (cm^{-1})	C=O (cm^{-1})	C=C (cm^{-1})	C-N (cm^{-1})	C-O (cm^{-1})
S4	-	2922	1700	1503, 1394	1368	1027
S6	3319	2964	1632	1502	1360	1056

5. Polymer Synthesis.

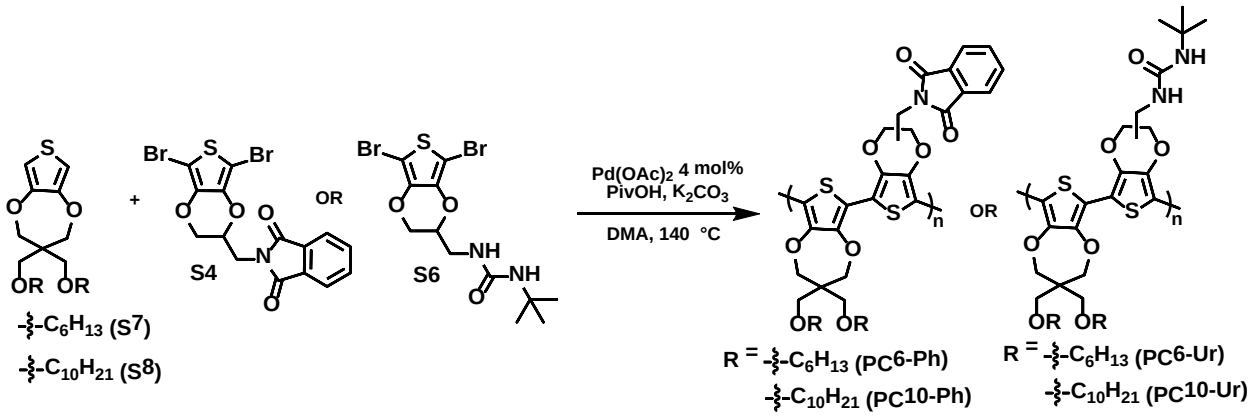

Scheme S2. Polymer synthesis via DArP.

General Procedure for DArP polymerization. An oven-dried 50 mL Schlenk tube with a stir bar was cooled under nitrogen. This was followed by the addition of S7 or S8 (0.23 mmol 1.0 equiv.) and S4 or S6 (0.23 mmol, 1.0 equiv.), PivOH (0.07 mmol, 0.3 equiv.), K_2CO_3 (0.58 mmol, 2.5 equiv.), and $Pd(OAc)_2$ (0.01 mmol, 0.04 equiv.) under nitrogen and the vessel was vacuum-backfilled with N_2 three times. Then, 2.3 mL of anhydrous DMA was added to the mixture and stirred for 10 min at room temperature to dissolve the monomers. The Schlenk flask was then placed into a pre-heated oil bath (140 °C) for 24 h. After cooling at room temperature, polymer solids were dissolved in chloroform, and the reaction mixture was precipitated into the chilled hexanes with rapid stirring. The polymer product was then filtered into a cellulose thimble and purified via Soxhlet extraction (hexanes, MeOH, and chloroform). The chloroform fraction was concentrated and precipitated into chilled hexanes. The purple solid was then collected via filtration and dried overnight under vacuum.

PC6-Ph. Yield: 53%. MALDI-TOF: M_n = 3.5 kg/mol; $Đ$ = 1.05. ^{1}H-NMR ($C_2D_2Cl_4$, 80 °C, 400 MHz) δ (ppm): 7.85-7.72 (br, 4H), 4.19 (br, 5H), 3.63-3.49 (br, 12H), 1.57 (br, 4H), 1.36-1.34 (br, 12H), 0.95-0.92 (br, 6H). ATR-FTIR (neat) cm^{-1}: 2920 (s), 2848 (s), 1736 (m), 1529 (m), 1411 (m), 1225 (m), 1086 (m).

PC6-Ur. Yield: 81%. MALDI-TOF: M_n = 2.97 kg/mol; $Đ$ = 1.02. ^{1}H-NMR ($C_2D_2Cl_4$, 80 °C, 400 MHz) δ (ppm): 4.71-3.97 (br, 5H), 3.80-3.25 (br, 12H), 1.64-1.50 (br, 4H), 1.32 (br, 21H), 0.95-

0.91 (br, 6H). ATR-FTIR (neat) cm^{-1}: 3330 br, w), 2922 (m), 2851 (m), 1651 (m), 1430 (s), 1325 (s), 1128 (m).

PC10-Ph. Yield: 52%. MALDI-TOF: M_n = 3.6 kg/mol; $Đ$ = 1.08. ^{1}H-NMR ($C_2D_2Cl_4$, 80 °C, 400 MHz) δ (ppm): 7.84-7.73 (br, 4H), 4.22-4.17 (br, 5H), 3.62-3.49 (br, 12H), 1.55 (br, 4H), 1.47-1.27 (br, 28H), 0.95 (br, 12H). ATR-FTIR (neat) cm^{-1}: 2919 (s), 2849 (s), 1736 (w), 1540 (m), 1408 (m), 1229 (m), 1110 (w).

PC10-Ur. Yield: 51%. MALDI-TOF: M_n = 3.2 kg/mol; $Đ$ = 1.03. ^{1}H-NMR ($C_2D_2Cl_4$, 80 °C, 400 MHz) δ (ppm): 4.71-3.97 (br, 5H), 3.80-3.25 (br, 12H), 1.64-1.50 (br, 4H), 1.32 (br, 37H), 0.95-0.91 (br, 6H). ATR-FTIR (neat) cm^{-1}: 3365, 2918, 2849, 1666, 1431, 1325, 1125.

6. Polymer ATR-FTIR.

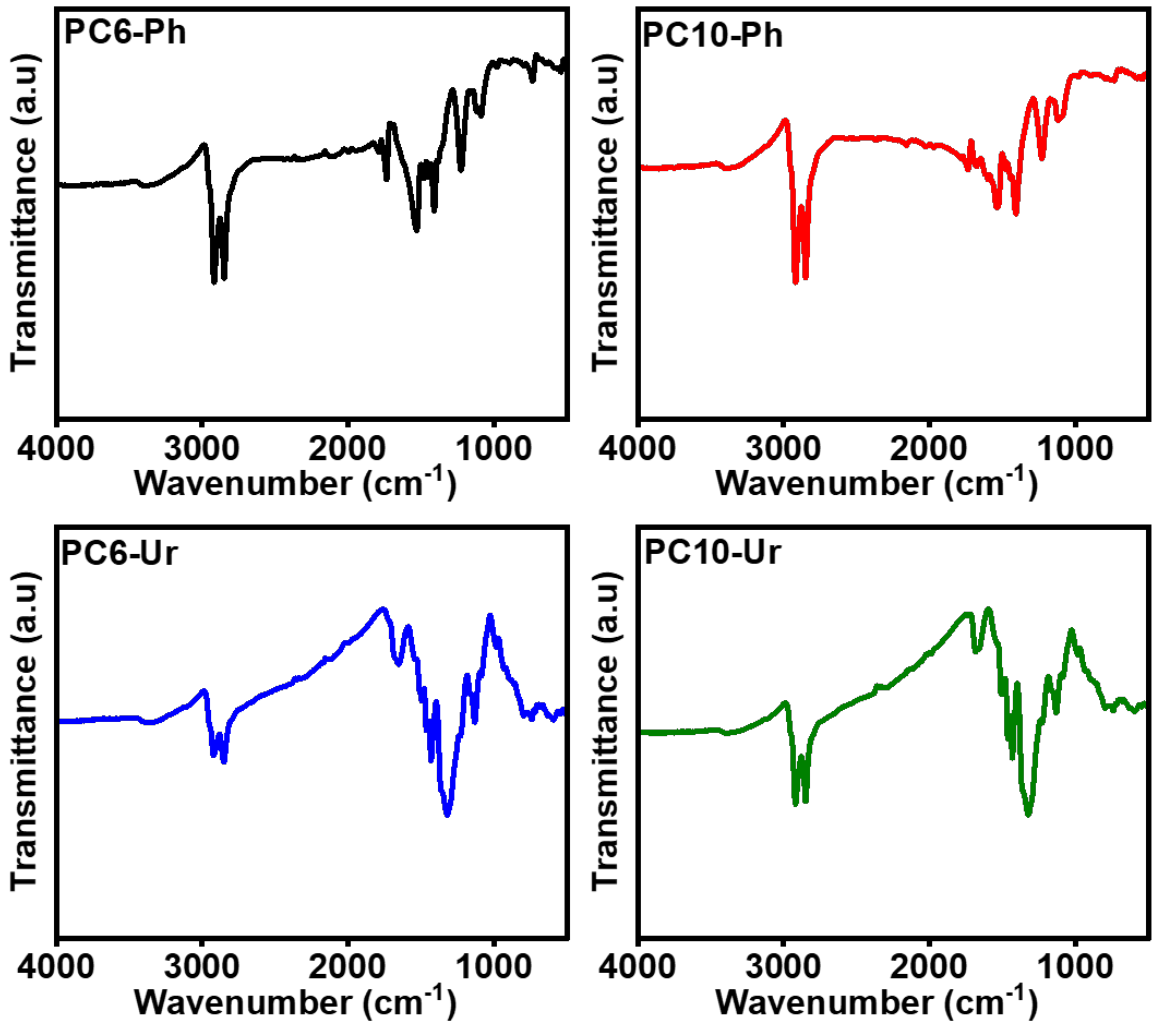

Figure S12. ATR-FTIR spectra of polymers PC6-Ph, PC10-Ph, PC6-Ur, and PC10-Ur.

Table S2.

Entry	N-H (cm^{-1})	C-H (cm^{-1})	C=O (cm^{-1})	C=C (cm^{-1})	C-N (cm^{-1})	C-O (cm^{-1})
PC6-Ph	-	2920, 2848	1736	1529, 1411	1225	1086
PC10-Ph	-	2919, 2849	1736	1540, 1408	1229	1110
PC6-Ur	3330	2922, 2851	1651	1430	1325	1128
PC10-Ur	3365	2918, 2849	1666	1431	1325	1125

7. Polymer NMR.

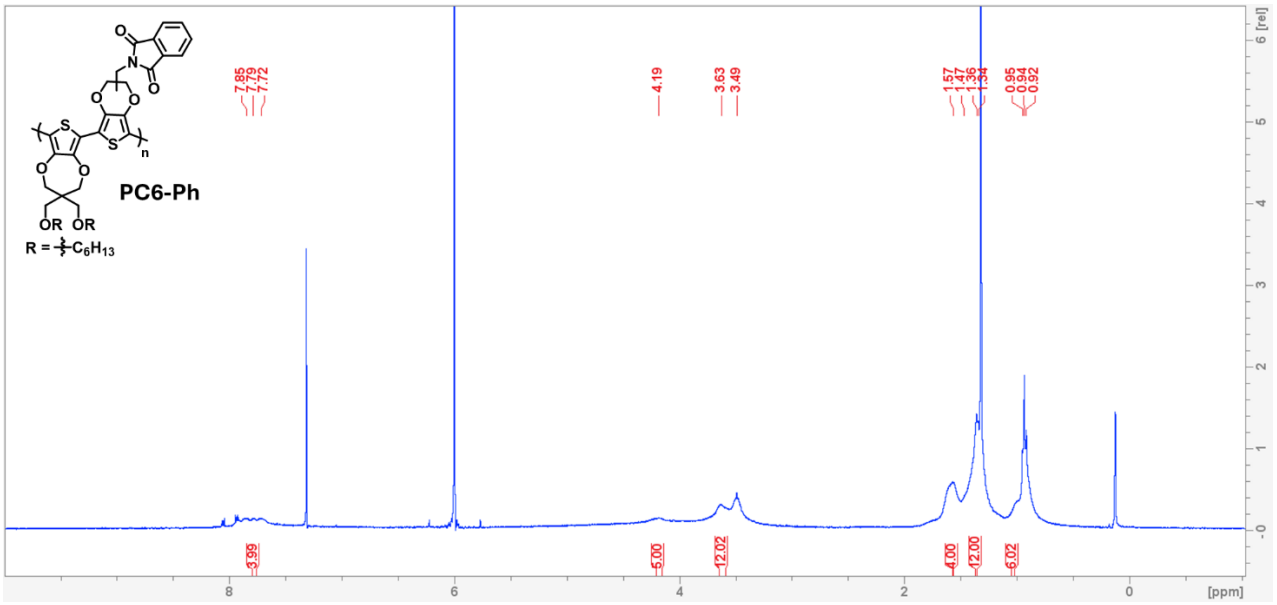

Figure S13. ^{1}H-NMR of PC6-Ph collected in $C_2D_2Cl_4$ at 80 °C and 400 MHz.

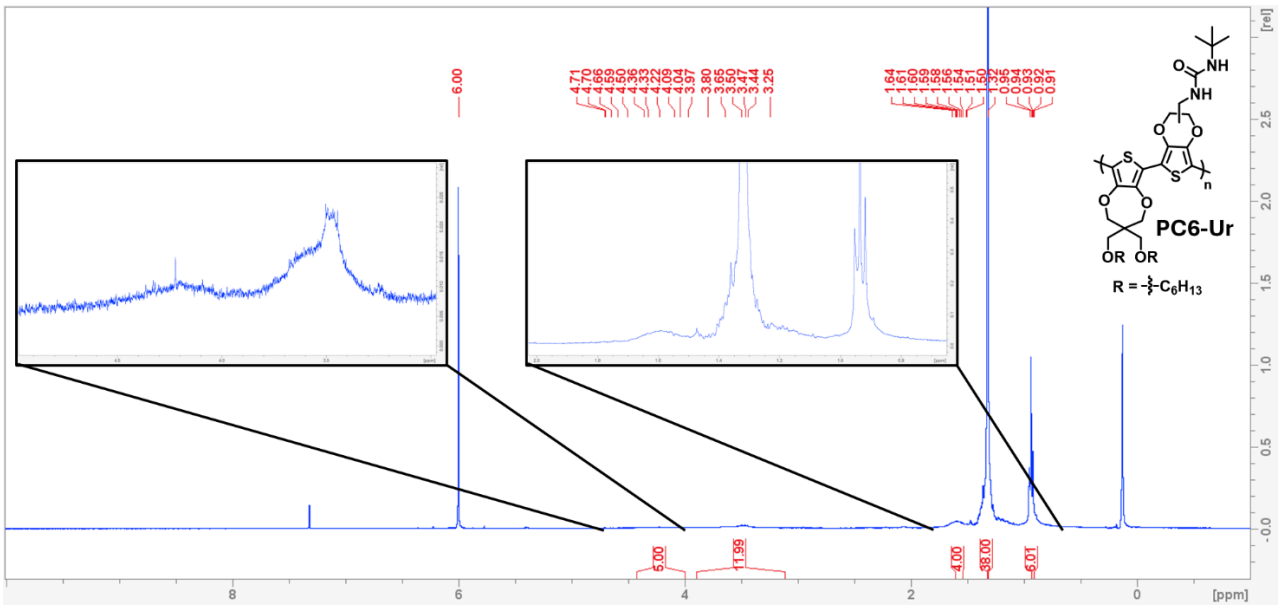

Figure S14. ^{1}H-NMR of PC6-Ur collected in $C_2D_2Cl_4$ at 80 °C and 400 MHz.

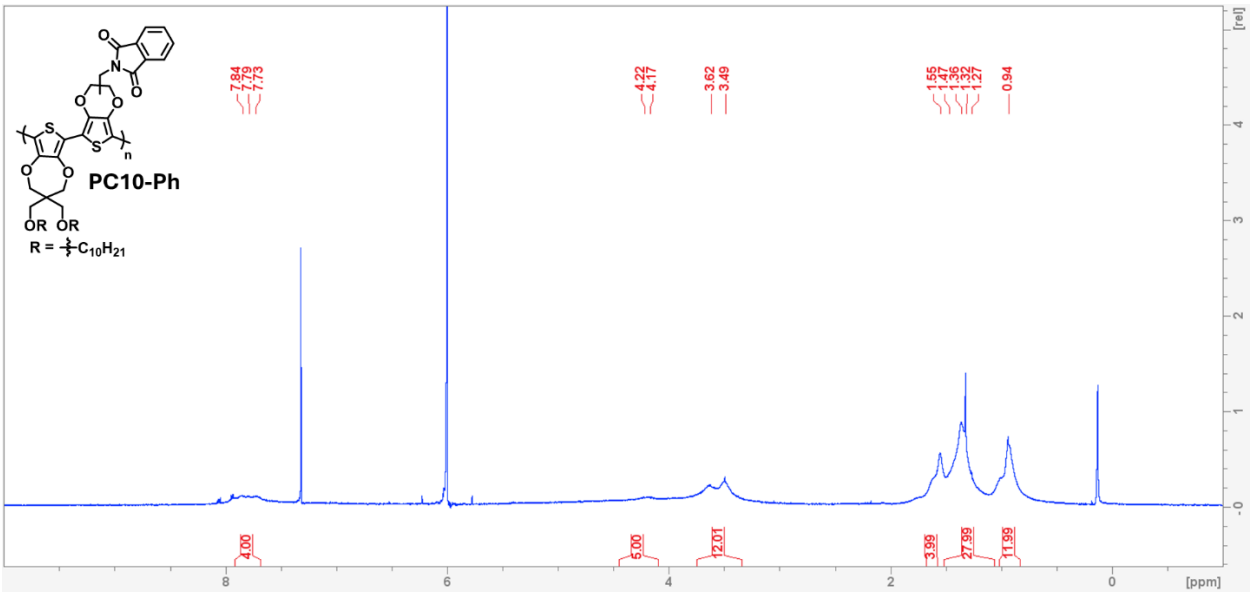

Figure S15. ^{1}H-NMR of PC10-Ph collected in $C_2D_2Cl_4$ at 80 °C and 400 MHz.

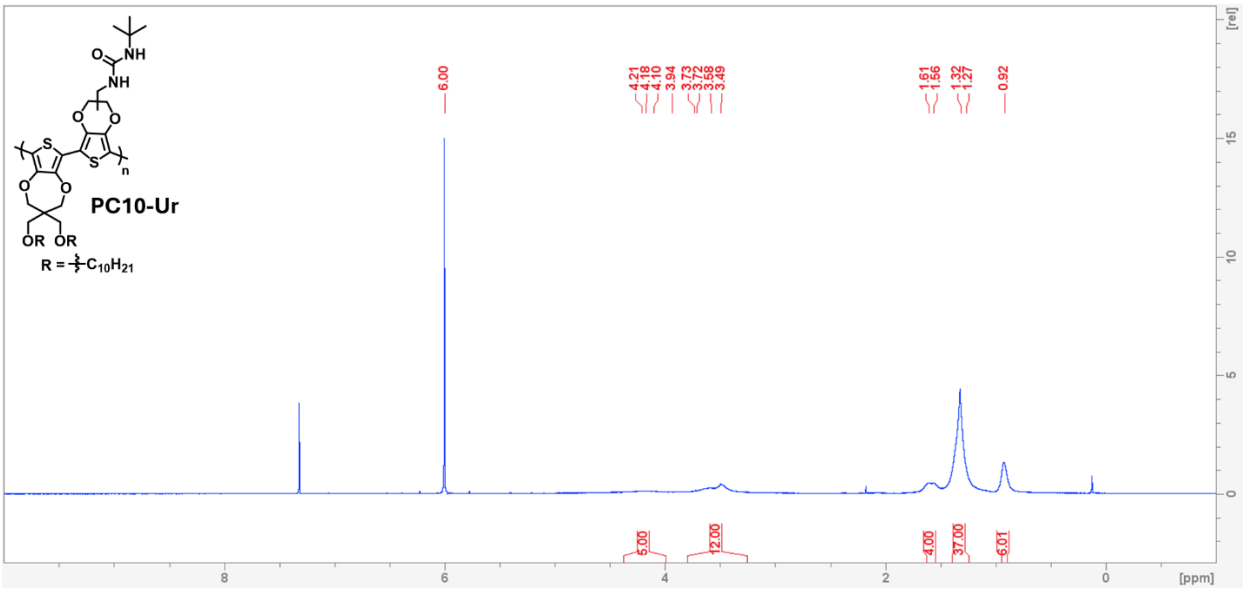

Figure S16. ^{1}H-NMR of PC10-Ph collected in $C_2D_2Cl_4$ at 80 °C and 400 MHz.

8. Thermogravimetric Analysis.

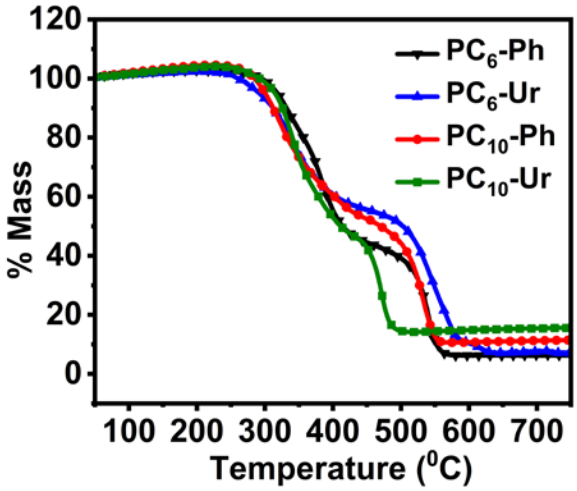

Figure S17. TGA thermograms for PC6-Ph, PC6-Ur, PC10-Ph, and PC10-Ur.

9. MALDI-TOF.

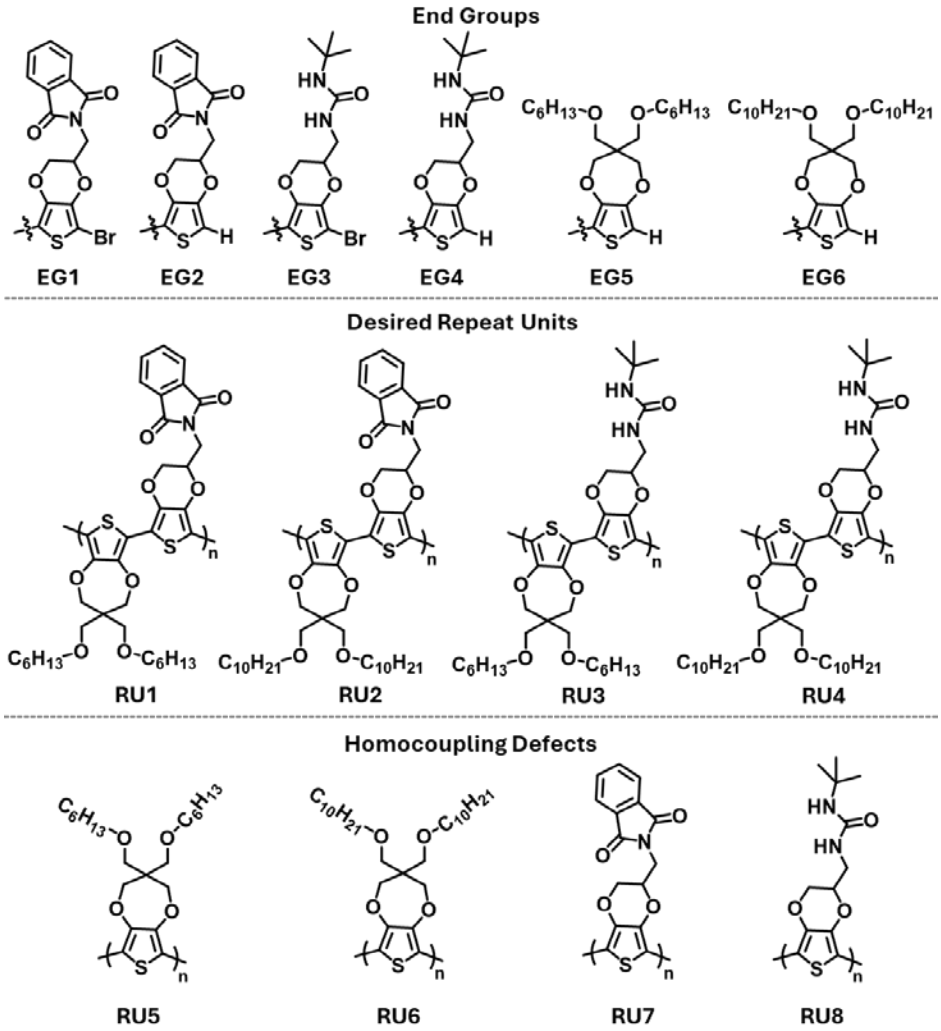

Figure S18. Proposed end-groups and repeat units present in MALDI-TOF spectra.

Table S3. Tabulated masses for the end groups and repeat units provided in Figure S18.

End Groups						
Identity	EG1	EG2	EG3	EG4	EG5	EG6
Mass	379.20	300.31	348.24	269.30	292.13	213.23
Desired Repeat Units						
Identity	RU1	RU2	RU3	RU4	-	-
Mass	681.86	794.07	650.89	763.11	-	-
Homocoupling Defects						
Identity	RU5	RU6	RU7	RU8	-	-
Mass	382.56	494.77	299.30	268.33	-	-

10. Contact Angle Measurements.

Contact angle measurements were performed using a rame-hart goniometer controlled by Pylon Viewer software. Polymer films for the measurements were fabricated using 30 mg/mL $CHCl_3$ solutions stirred overnight at 65 °C followed by spincoating (3000 rpm) onto glass-ITO substrates. 5 μL of DI-H_2O or ethylene glycol were used for each measurement. Images were then processed using ImageJ software equipped with the DropSnake plugin.

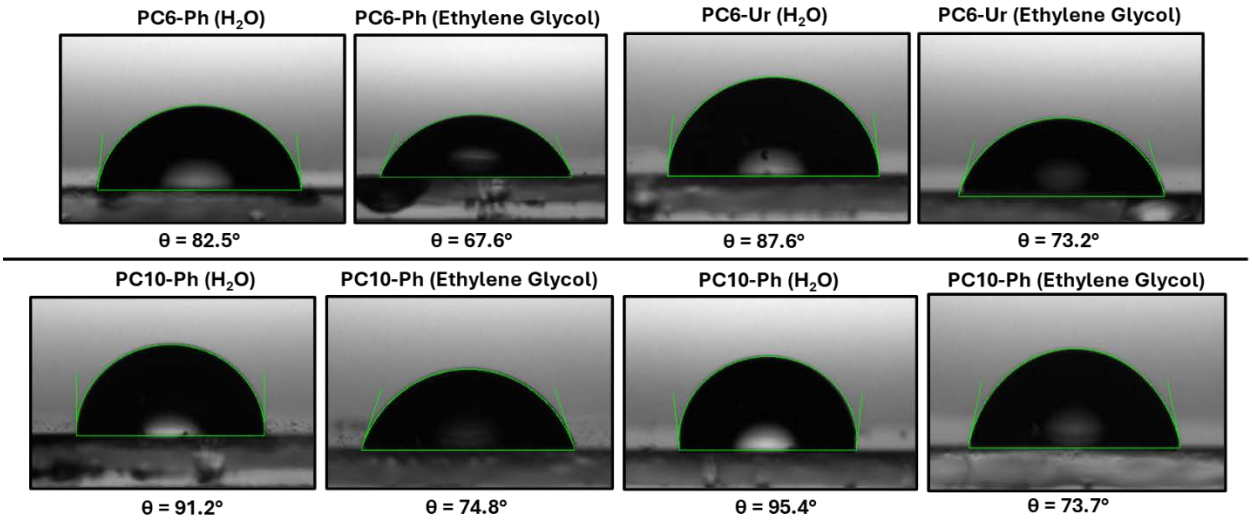

Figure S19. Contact angle measurements for polymers PC6-Ph, PC6-Ur, PC10-Ph, and PC10-Ph using ethylene glycol and water.

11. Density Functional Theory (DFT) Calculations.

Calculations were carried out in the frame of density functional theory (DFT) using Gaussian 09 with the B3LYP functional together with 6-31G*(d) basis set, which has been implemented for similar compounds.[4] Model compounds were based on repeat units for the polymers with the alkyl substituents replaced with methyl substituents to simplify the calculations. Molecular orbital distributions were visualized using AMPAC 11 molecular modelling software.

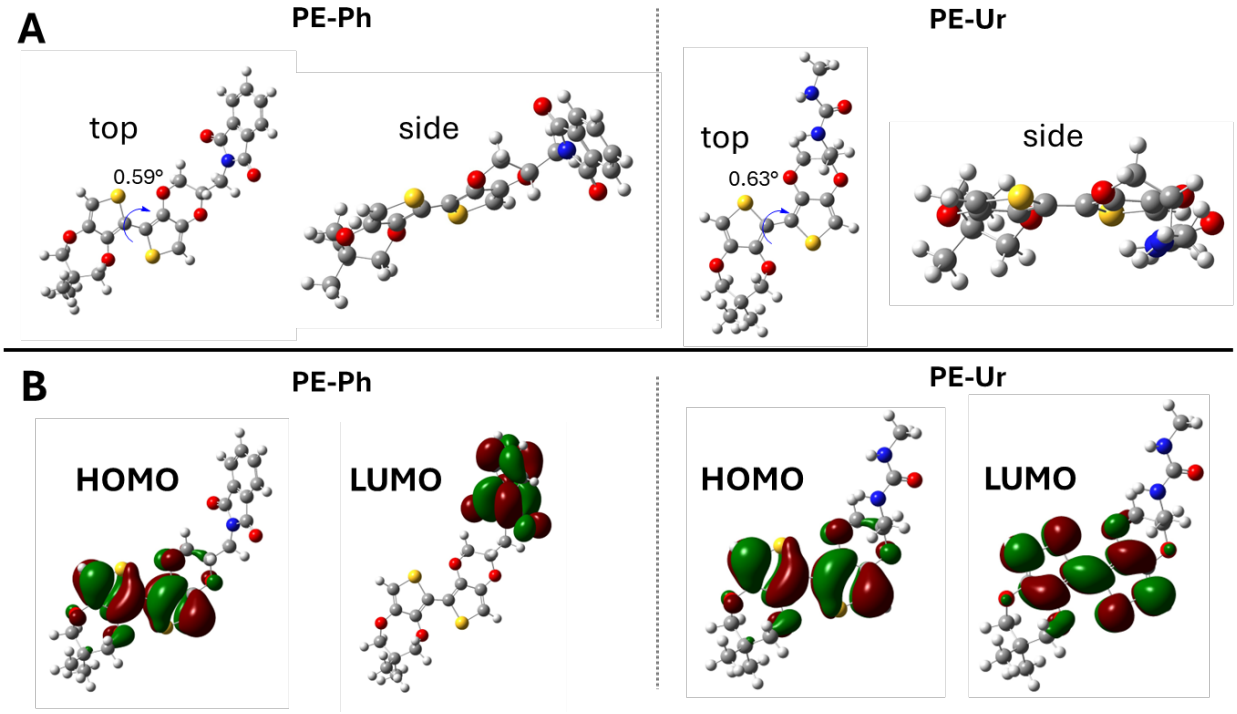

Figure S20. Geometry optimizations (A) and HOMO/LUMO orbital distributions (B) for the model compounds PE-Ph and PE-Ur.

Table S4. Calculated HOMO/LUMO energy levels and bandgaps (E_g) for the model compounds PE-Ph and PE-Ur.

Model Compound	HOMO (eV)	LUMO (eV)	E_g (eV)
PE-Ph	-5.11	-2.78	-2.33
PE-Ur	-5.20	-1.11	-4.09

12. Cyclic Voltammetry.

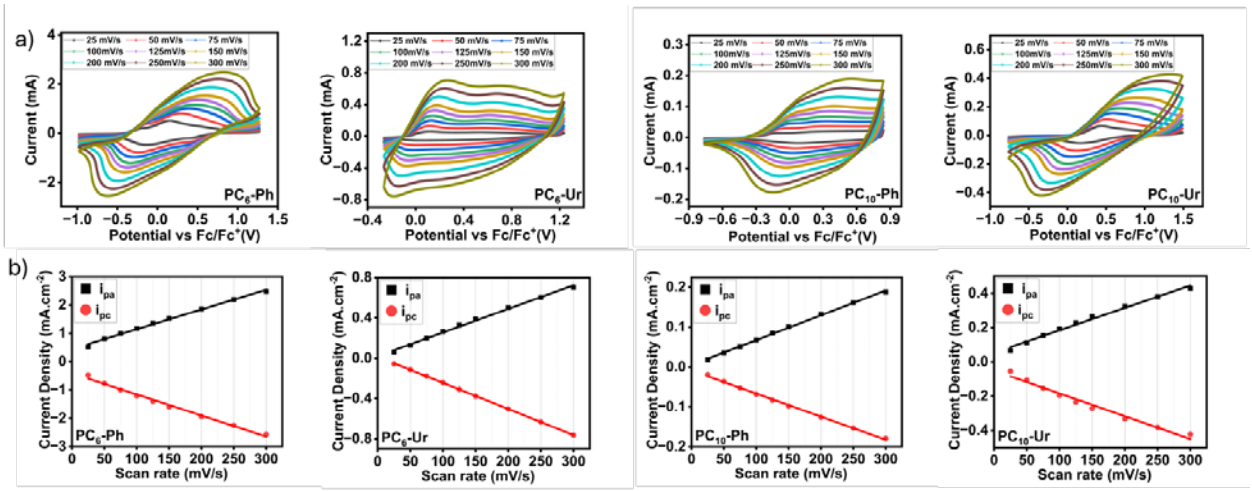

Figure S21: (a) Cyclic-voltammetry measurements with different scan rates (25, 50, 75, 100, 125, 150, 200, 250, and 300 mV/s) of PC6-Ph, PC6-Ur, PC10-Ph, and PC10-Ur in 0.1 M $LiPF_6$/PC electrolyte. Referenced to the Fc/Fc^+ redox couple. (b) i_{pc}/i_{pa} as a function of scan-rate of PC6-Ph, PC6-Ur, PC10-Ph, and PC10-Ur.

Table S5. Anodic/Cathodic peak current (*i*pa/*i*pc) as a function of voltage scan-rate for PC6-Ph.

Polymer	Scan Rate ($mV \cdot s^{-1}$)	*i*pa ($mA \cdot cm^{-2}$)	*i*pc ($mA \cdot cm^{-2}$)
PC6-Ph	25	0.52173	-0.47538
	50	0.80306	-0.7725
	75	0.98981	-0.99491
	100	1.16868	-1.20543
	125	1.35993	-1.39728
	150	1.53311	-1.59423
	200	1.86078	-1.94058
	250	2.19525	-2.24958
	300	2.47368	-2.56537

Table S6. Anodic/Cathodic peak current (*i*pa/*i*pc) as a function of voltage scan-rate for PC6-Ur.

Polymer	Scan Rate ($mV \cdot s^{-1}$)	*i*pa ($mA \cdot cm^{-2}$)	*i*pc ($mA \cdot cm^{-2}$)
PC6-Ur	25	0.05908	-0.05552
	50	0.12733	-0.11409
	75	0.1966	-0.17827
	100	0.26435	-0.24092
	125	0.32852	-0.30815
	150	0.38862	-0.37640
	200	0.49864	-0.50374
	250	0.60255	-0.63260
	300	0.7039	-0.76299

Table S7. Anodic/Cathodic peak current (*i*pa/*i*pc) as a function of voltage scan-rate for PC10-Ph.

Polymer	Scan Rate (mV·s^{-1})	*i*pa (mA·cm^{-2})	*i*pc (mA·cm^{-2})
PC10-Ph	25	0.01846	-0.01948
	50	0.03502	-0.03654
	75	0.05093	-0.05259
	100	0.06800	-0.06851
	125	0.08480	-0.08353
	150	0.10059	-0.09792
	200	0.13254	-0.12606
	250	0.16070	-0.15306
	300	0.18795	-0.17903

Table S8. Anodic/Cathodic peak current (*i*pa/*i*pc) as a function of voltage scan-rate for PC10-Ur.

Polymer	Scan Rate (mV·s^{-1})	*i*pa (mA·cm^{-2})	*i*pc (mA·cm^{-2})
PC10-Ur	25	0.06621	-0.05433
	50	0.11319	-0.1064
	75	0.15478	-0.15422
	100	0.19242	-0.19553
	125	0.22779	-0.23486
	150	0.26316	-0.27136
	200	0.32456	-0.33164
	250	0.38031	-0.38144
	300	0.42784	-0.42218

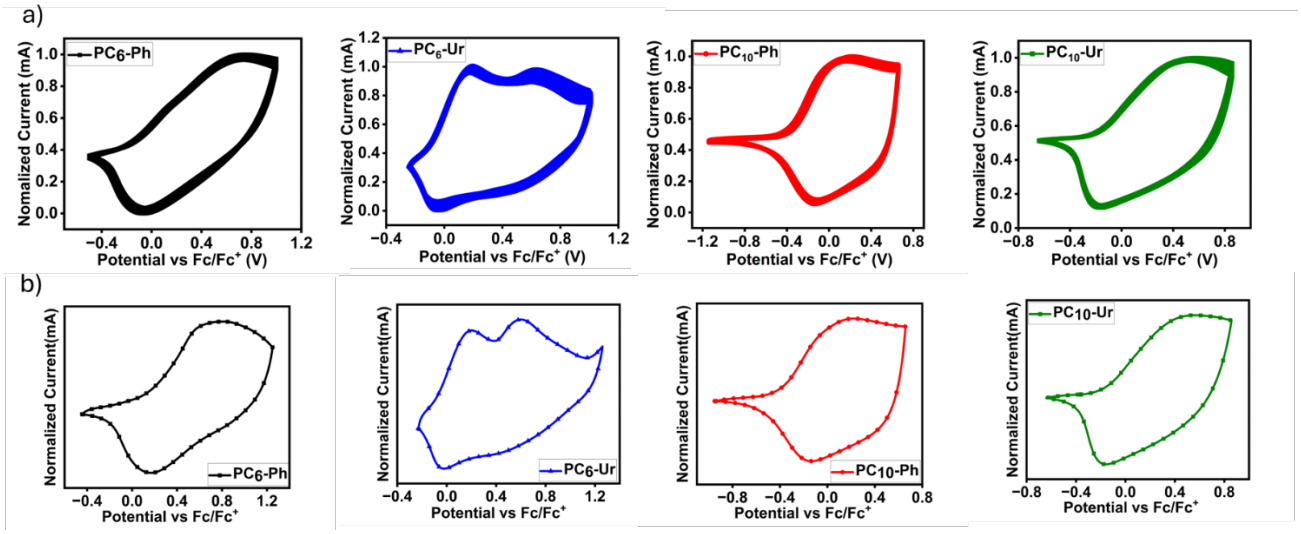

Figure S22. (a) Electrochemical stability measurements of PC6-Ph, PC6-Ur, PC10-Ph, and PC10-Ur (100 cycles in 0.1 M $LiPF_6$/PC electrolyte with a scan rate 100 mV/s). Referenced to the Fc/Fc^+ redox couple. (b) CV voltammograms used for calculating the specific capacitances of PC6-Ph, PC6-Ur, PC10-Ph, and PC10-Ur in 0.1 M $LiPF_6$/PC electrolyte.

13. Electrochromic Characterization.

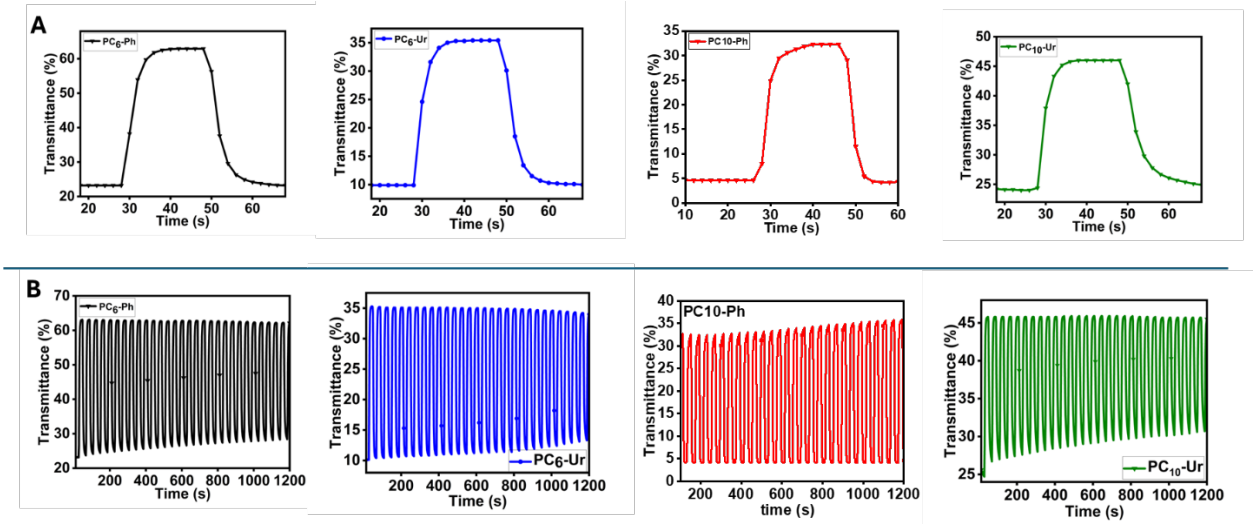

Figure S23. Electrochromic cycling stability (a) and switching dynamics (b) for PC6-Ph (black), PC6-Ur (blue), PC10-Ph (red), and PC10-Ur (green) collected in 0.5 M $LiPF_6$/PC

Table S9. CIELAB chromaticity coordinates for the neutral and oxidized forms of PC6-Ph, PC6-Ur, PC10-Ph, and PC10-Ur.

Polymer	*L*	a	b
PC6-Ph neutral	47	11	-29
PC6-Ph oxidized	77	-1	-2
PC6-Ur neutral	60	25	-9
PC6-Ur oxidized	77	-1	-2
PC10-Ph neutral	45	10.6	-26.3
PC10-Ph oxidized	81	1.4	11.6
PC10-Ur neutral	22	3.7	-31
PC10-Ur oxidized	55	-3.7	-4

14. Atomic Force Microscopy.

Atomic force microscopy (AFM) was measured on a Digital Instrument Veeco AFM in standard tapping mode using a Si-cantilever.[5] Polymer films were prepared at the concentration of 30mg/ml in $CHCl_3$ solution and stirred overnight at 65°C. The polymer solution was then spin coated at 2500 rpm onto 2×2 cm pre-cut glass substrates. The set point for all films is fixed within range of 0.70 to 1.5 nA magnitude with integral and proportional gains of 0.1 and 0.2 respectively. The scan speed is constant at 0.5 Hz in tapping mode. Nasoscope 6.13r1 and WSxM 5.0 software was used to acquire and analyze data respectively.

15. Scanning Electron Microscopy.

Scanning electron microscopy was performed using a High-resolution Scanning Electron Microscope (SEM) SU-4800 (Hitachi, Japan) under 10 KV of acceleration voltage to analyze the polymer films. Polymer films were prepared as described in the AFM section. Prior to imaging, the samples were coated with Au and attached to the sample holder using Cu tape, and the images were collected following published procedures.[2]

16. References.

(1) Zubair, T.; Ramos, R. S.; Morales, A.; Pankow, R. M. Synthesis of Poly(3,4-Propylenedioxythiophene) (PProDOT) Analogues *via* Mechanochemical Oxidative Polymerization. *Polym. Chem.* **2025**, 10.1039.D4PY01253D. https://doi.org/10.1039/D4PY01253D.

(2) Mahmud, M. S.; Delgadillo, A.; Urbay, J. E. M.; Hassan, M. S.; Zaman, S.; Dieguez, D.; Fontes, D.; Leyva, D.; Dantzler, J.; Lopez, A.; Joyce, S. N.; Roberson, D. A.; Michael, K.; Lin, Y.; Marchi, A. N.; Schuster, B. E. Chemical Aging and Degradation of Stereolithographic 3D-Printed Material: Effect of Printing and Post-Curing Parameters. *Polymer Degradation and Stability* **2025**, *232*, 111151. https://doi.org/10.1016/j.polymdegradstab.2024.111151.

(3) Liu, J.; Hou, W.; Tang, D.; Gao, Y.; Yao, S.; Jiang, L.; Zhang, Z.; Ouyang, M.; Zhang, C. Donor–Node–Acceptor Ambipolar Conducting Polymer Electrode Materials for Wide-Voltage and High-Stability Supercapacitors. *ACS Sustainable Chem. Eng.* **2022**, *10* (48), 15978–15986. https://doi.org/10.1021/acssuschemeng.2c05441.

(4) Liu, J.; Hou, W.; Tang, D.; Gao, Y.; Yao, S.; Jiang, L.; Zhang, Z.; Ouyang, M.; Zhang, C. Donor–Node–Acceptor Ambipolar Conducting Polymer Electrode Materials for Wide-Voltage and High-Stability Supercapacitors. *ACS Sustainable Chem. Eng.* **2022**, *10* (48), 15978–15986. https://doi.org/10.1021/acssuschemeng.2c05441.

(5) Ramos, R. S.; Muñoz-Alba, F.; Saini, K.; Castaneda, K. M.; Juarez-Rangel, V. F.; Sreenivasan, S. T.; Ruiz Delgado, M. C.; Ponce Ortiz, R.; Pankow, R. M. Harnessing the Reversible Isomerization of Spiropyran to Merocyanine in Conjugated Polymers for Broadband Ultra-Violet to near-Infrared Electrochromic Switching. *J. Mater. Chem. C* **2025**, *13* (25), 12772–12782. https://doi.org/10.1039/D5TC01125F.